

## AXIONS AND THEIR DISTRIBUTION IN GALACTIC HALOS

P. SIKIVIE

*Department of Physics,  
University of Florida,  
Gainesville, FL 32611-8440  
E-mail: sikivie@phys.ufl.edu*

Axion physics is briefly reviewed. Constraints from laboratory searches, astrophysics and cosmology require the axion mass to be in the range  $10^{-6} \lesssim m_a < 3 \cdot 10^{-3} \text{eV}$ . Near the lower end of this range, axions are all or a major component of the cold dark matter of the universe. The late infall of axions, and of any other cold dark matter particles, onto our galaxy produces streams and caustics in its halo. The outer caustics are topological spheres whereas the inner caustics are rings. The self-similar model of galactic halo formation predicts that the caustic ring radii  $a_n$  obey the approximate law  $a_n \sim 1/n$ . Evidence for this law has been found in a statistical study of 32 extended and well-measured external galactic rotation curves, and in the existence and distribution of sharp rises in the Milky Way rotation curve. Moreover, a triangular feature in the IRAS map of the Galactic plane is consistent with the imprint of a ring caustic upon the baryonic matter. Its position coincides with a rise in the rotation curve, the one nearest to us. These observations imply that the dark matter in our neighborhood is dominated by a single flow. Estimates of that flow's density and velocity vector are given.

### 1. Axions

The axion was postulated approximately 25 years ago<sup>1</sup> to explain why the strong interactions conserve P and CP in spite of the violation of those symmetries by the weak interactions. The QCD Lagrangian

$$L_{QCD} = -\frac{1}{4}G_{\mu\nu}^a G^{a\mu\nu} + \sum_{j=1}^n \left[ \bar{q}_j \gamma^\mu i D_\mu q_j - (m_j q_{Lj}^\dagger q_{Rj} + \text{h.c.}) \right] + \frac{\theta g^2}{32\pi^2} G_{\mu\nu}^a \tilde{G}^{a\mu\nu} \quad . \quad (1)$$

violates P and CP unless  $\theta = 0 \pmod{\pi}$ . The absence of P and CP violations in the strong interactions, in particular the experimental bound on the neutron electric dipole moment, yields the limit:  $\theta < 10^{-9}$ . However,

in the Standard Model of particle physics, because of P and CP violation by the weak interactions, one would expect  $\theta$  to be of order one. This discrepancy is called the 'strong CP problem'.

The existence of an axion solves this problem in a simple manner which is rich in implications for experiment, for astrophysics and for cosmology. In axion models, the  $\theta$ -parameter in Eq. (1) is replaced by

$$\theta_{\text{eff}} = \theta + \frac{a(x)}{f_a} \quad (2)$$

where  $a(x)$  is the axion field and  $f_a$ , called the axion decay constant, is of order the energy scale at which the U(1) symmetry of Peccei and Quinn is spontaneously broken. The axion is the quasi-Nambu-Goldstone boson associated with this symmetry breaking. In axion models, the effective value of  $\theta$ , Eq. (2), relaxes to zero dynamically. The axion mass is given in terms of  $f_a$  by

$$m_a \simeq 6 \mu\text{eV} \frac{10^{12}\text{GeV}}{f_a}. \quad (3)$$

The axion has zero spin, zero electric charge, and negative intrinsic parity. All its couplings are inversely proportional to  $f_a$ . Of particular relevance to present axion searches is its coupling to two photons:

$$L_{a\gamma\gamma} = -g_\gamma \frac{\alpha a(x)}{\pi f_a} \vec{E} \cdot \vec{B} \quad (4)$$

where  $\vec{E}$  and  $\vec{B}$  are the electric and magnetic fields,  $\alpha$  is the fine structure constant, and  $g_\gamma$  is a model-dependent coefficient of order one.

The axion mass is not known a-priori. Indeed the axion solves the strong CP problem for any value of its mass. However masses larger than 50 keV are ruled out by searches for the axion in high energy and nuclear physics experiments. Also, masses between 300 keV and 3 milli-eV are ruled out by stellar evolution, specifically the ages of red giants and the duration of the observed neutrino pulse from Supernova 1987a. Finally, masses less than about one micro-eV are ruled out because axions that light would be so abundantly produced in the early universe as to exceed the closure density. In summary, the only remaining window of allowed axions masses is  $10^{-6} \lesssim m_a < 3 \cdot 10^{-3}\text{eV}$ .

In that window, axions contribute importantly to the present cosmological energy density. Axions are one of the leading cold dark matter candidates. Dark matter axions can be searched for on Earth by stimulating their conversion to micro-wave photons in an electromagnetic cavity

permeated by a strong magnetic field <sup>2</sup>. Searches of this type are presently under way in the US <sup>3</sup> and in Japan <sup>4</sup>. The method of axion to photon conversion in a magnetic field can also be applied to solar axion detection <sup>2,5</sup>. A limit was published this year by Minowa's group <sup>6</sup> in Tokyo. Also the CAST experiment at CERN <sup>7</sup>, using a decommissioned LHC magnet, is getting ready to take data.

The ADMX experiment at Lawrence Livermore Laboratory, which searches for dark matter halo axions, is described by D. Kinion at this meeting. If it discovers a signal, the detector will be able to measure the kinetic energy spectrum of cold dark matter with great precision and resolution. The spectrum of axions and WIMPs is the same, in the (excellent) approximation where the primordial velocity dispersion of both cold dark matter candidates is neglected, because it is the outcome of purely gravitational interactions. My collaborators and I have been motivated to try and predict this spectrum. It has been an exciting adventure which I report on in the rest of my talk.

## 2. Flows and Caustics of Dark Matter

The model of the structure of the halos of isolated galaxies which we have developed is based on the observation that the dark matter particles must lie on a 3-dimensional sheet in phase-space, that this sheet cannot break, and hence that its evolution is constrained by topology. The thickness of the sheet is the velocity dispersion. The primordial velocity dispersion of the leading cold dark matter candidates is extremely small, of order  $10^{-12}c$  for WIMPs and  $3 \cdot 10^{-17}c$  (at most) for axions. For a coarse-grained observer the sheet may have additional velocity dispersion because it is wrapped up on scales which are small compared to the galaxy as a whole. This latter effective velocity dispersion is associated with the clumpiness of the dark matter before it falls onto the galaxy. The effective velocity dispersion of the infalling dark matter must be much less than the rotation velocity of the galaxy for the model to have validity, say less than 30 km/s for our galaxy. On the other hand, by comparing the model with observations, an upper bound of order 50 m/s has been obtained, as described below.

Where a galaxy forms, the sheet wraps up in phase-space, turning clockwise in any two dimensional cut  $(x, \dot{x})$  of that space.  $x$  is the physical space coordinate in an arbitrary direction and  $\dot{x}$  its associated velocity. The outcome of this process is a discrete set of flows at any physical point in a galactic halo <sup>8</sup>. Two flows are associated with particles falling through the

galaxy for the first time ( $n = 1$ ), two other flows are associated with particles falling through the galaxy for the second time ( $n = 2$ ), and so on. Scattering in the gravitational wells of inhomogeneities in the galaxy (e.g. molecular clouds and globular clusters) are ineffective in thermalizing the flows with low values of  $n$ .

Caustics appear wherever the projection of the phase-space sheet onto physical space has a fold<sup>9,10,11,12</sup>. Generically, caustics are surfaces in physical space. On one side of the caustic surface there are two more flows than on the other. At the surface, the dark matter density is very large. It diverges there in the limit of zero velocity dispersion. There are two types of caustics in the halos of galaxies, inner and outer. The outer caustics are topological spheres surrounding the galaxy. They are located near where a given outflow reaches its furthest distance from the galactic center before falling back in. The inner caustics are rings<sup>9</sup>. They are located near where the particles with the most angular momentum in a given inflow reach their distance of closest approach to the galactic center before going back out. A caustic ring is a closed tube whose cross-section is a  $D_{-4}$  (also called *elliptic umbilic*) catastrophe<sup>12</sup>. The existence of these caustics and their topological properties are independent of any assumptions of symmetry.

Primordial peculiar velocities are expected to be the same for baryonic and dark matter particles because they are caused by gravitational forces. Later the velocities of baryons and CDM differ because baryons collide with each other whereas CDM is collisionless. However, because angular momentum is conserved, the net angular momenta of the dark matter and baryonic components of a galaxy are aligned. Since the caustic rings are located near where the particles with the most angular momentum in a given infall are at their closest approach to the galactic center, they lie close to the galactic plane.

### 3. A Formula for the Caustic Ring Radii

A specific proposal has been made for the radii  $a_n$  of caustic rings<sup>9</sup>:

$$\{a_n : n = 1, 2, \dots\} \simeq (39, 19.5, 13, 10, 8, \dots)\text{kpc} \\ \times \left(\frac{j_{\max}}{0.25}\right) \left(\frac{0.7}{h}\right) \left(\frac{v_{\text{rot}}}{220\frac{\text{km}}{\text{s}}}\right) \quad (5)$$

where  $h$  is the present Hubble constant in units of 100 km/(s Mpc),  $v_{\text{rot}}$  is the rotation velocity of the galaxy and  $j_{\max}$  is a parameter with a specific value for each halo. For large  $n$ ,  $a_n \sim 1/n$ . Eq. 5 is predicted by the

self-similar infall model<sup>13,14</sup> of galactic halo formation.  $j_{\max}$  is then the maximum of the dimensionless angular momentum  $j$ -distribution<sup>14</sup>. The self-similar model depends upon a parameter  $\epsilon$ <sup>13</sup>. In CDM theories of large scale structure formation,  $\epsilon$  is expected to be in the range 0.2 to 0.35<sup>14</sup>. Eq. 5 is for  $\epsilon = 0.3$ . However, in the range  $0.2 < \epsilon < 0.35$ , the ratios  $a_n/a_1$  are almost independent of  $\epsilon$ . When  $j_{\max}$  values are quoted below,  $\epsilon = 0.3$  and  $h = 0.7$  will be assumed.

Since the caustic rings lie close to the galactic plane, they cause bumps in the rotation curve, at the locations of the rings. In ref. [15] a set of 32 extended well-measured rotation curves was analyzed and statistical evidence was found for bumps distributed according to Eq. 5. That study suggests that the  $j_{\max}$  distribution is peaked near 0.27. The rotation curve of NGC3198, one of the best measured, by itself shows three faint bumps which are consistent with Eq. 5 and  $j_{\max} = 0.28$ .

Because angular momentum has the effect of depleting the inner halo, an effective core radius is produced when angular momentum is included into the self-similar infall model<sup>14</sup>. The average amount of angular momentum of the Milky Way halo can be estimated by requiring that approximately half of the rotation velocity squared at our location is due to dark matter, the other half being due to baryonic matter. This yields  $\bar{j} \sim 0.2$  where  $\bar{j}$  is the average of the  $j$ -distribution for our halo<sup>14</sup>. If the  $j$ -distribution is taken to be that of a rigidly rotating sphere, we have  $j_{\max} = \frac{4}{\pi}\bar{j} \sim 0.254$ . The value which will be obtained below (0.263) from a fit to bumps in the Milky Way rotation curve is consistent with this earlier estimate.

#### 4. The Milky Way rotation curve

Galactic rotation curves are obtained from HI and CO surveys of the Galactic plane. A list of surveys performed to date is given in ref. [16]. The CO surveys have far better angular resolution than the HI surveys because their wavelength is nearly two orders of magnitude smaller (0.26 cm vs. 21 cm). The most detailed Galactic rotation curve appears to be that obtained<sup>17</sup> from the Massachusetts-Stony Brook North Galactic Plane CO survey<sup>18</sup>. It is reproduced in Fig. 1. It exhibits a series of ten sharp rises between 3 kpc and our own radius, taken to be 8.5 kpc.

The rises can be interpreted<sup>19</sup> as due to the presence of caustic rings of dark matter. The effect of a caustic ring in the plane of a galaxy upon its rotation curve was analyzed in ref. [12]. It was shown that the radius  $r_1$  where the rise starts should be identified with the caustic ring radius  $a_n$ , and

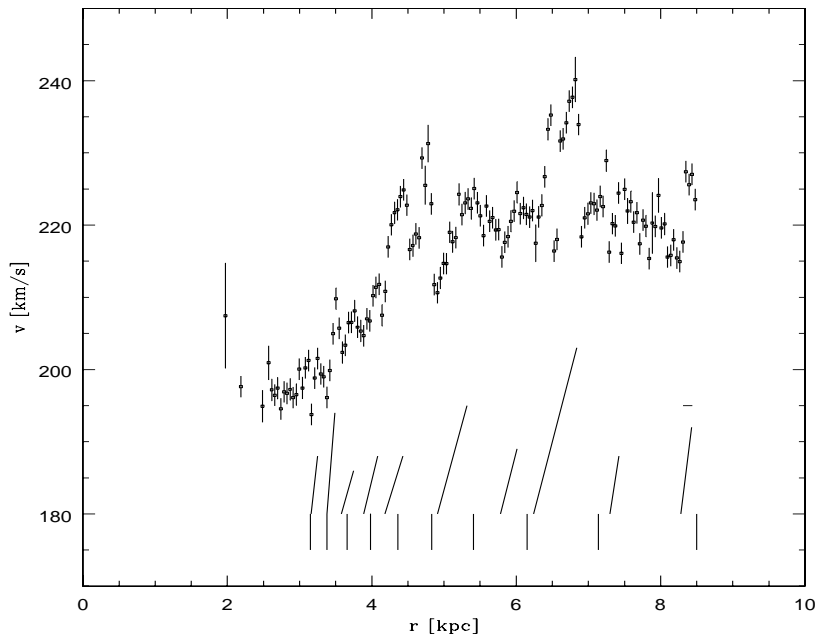


Figure 1. North Galactic rotation curve from ref. [17]. The locations of the rises are indicated by line segments parallel to the rises but shifted downwards. The caustic ring radii in the fit described in the text are shown as vertical line segments. The position of the triangular feature in the IRAS map of the galactic plane near  $80^\circ$  longitude is shown by the short horizontal line segment.

the radius  $r_2$  where the rise ends should be identified with  $a_n + p_n$  where  $p_n$  is the caustic ring width. The ring widths depend in a complicated way on the velocity distribution of the infalling dark matter at last turnaround<sup>12</sup> and are not predicted by the model. They also need not be constant along the ring. The rises between 3 and 7 kpc were fitted to the model prediction for the caustic ring radii, Eq. 5. For  $\epsilon = 0.3$  and  $j_{\max} = 0.263$ , one has  $rmsd \equiv \left[ \frac{1}{10} \sum_{n=5}^{14} \left( 1 - \frac{a_n}{r_{1n}} \right)^2 \right]^{\frac{1}{2}} = 3\%$ . So we find that, for model parameters

in the expected range, a sharp rise is present in the rotation curve for each of the caustic rings typically within 3% of the predicted radius.

In the past, rises (or bumps) in galactic rotation curves have been interpreted as due to the presence of spiral arms. However there are reasons to believe that the rises in the high resolution rotation curve of Fig. 1 are caused by caustic rings rather than spiral arms. First, there are of order ten rises in the range of radii covered (3 to 8.5 kpc) whereas the expected number of spiral arms is much less than ten. Only three spiral arms are known in that range: Scutum, Sagittarius and Local. On the other hand, the observed number of rises agrees with the number of caustic rings for the expected values<sup>14</sup> of the model parameters, e.g.  $\epsilon = 0.3$  and  $j_{\max} = 0.254$ . Second, the rises are sharp transitions in the rotation curve, both where they start ( $r_1$ ) and where they end ( $r_2$ ). One would expect spiral arms to produce smoother features. Sharp transitions are consistent with caustic rings because the latter have divergent density at  $r_1 = a$  and  $r_2 = a + p$  in the limit of vanishing velocity dispersion. Finally, there are bumps and rises in rotation curves measured at galactocentric distances much larger than the disk radius, where there are no spiral arms seen. In particular, the features found in the composite rotation curve constructed in ref. [9] are at distances 20 kpc and 40 kpc when scaled to our own galaxy. So there already exists evidence that some bumps or rises are not due to spiral arms.

## 5. Caustic Ring Imprint

The location of caustic rings may be revealed by the gas that they accrete. Looking tangentially to a ring caustic from a vantage point in the plane of the ring, one may recognize the tricusp<sup>12</sup> shape of the  $D_{-4}$  catastrophe. I searched for such features. The IRAS map of the galactic disk in the direction of galactic coordinates  $(l, b) = (80^\circ, 0^\circ)$  shows a triangular shape which is strikingly reminiscent of the cross-section of a ring caustic. The vertices of the triangle are at  $(l, b) = (83.5^\circ, 0.3^\circ)$ ,  $(77.3^\circ, 3.5^\circ)$  and  $(77.4^\circ, -2.7^\circ)$ . Images can be obtained from the Skyview Virtual Observatory (<http://skyview.gsfc.nasa.gov/>). The shape is correctly oriented with respect to the galactic plane and the galactic center. To an extraordinary degree of accuracy it is an equilateral triangle with axis of symmetry parallel to the galactic plane, as is expected for a caustic ring whose transverse dimensions are small compared to its radius. Moreover its position is consistent with the position of a rise in the rotation curve, the one between 8.28 and 8.43 kpc ( $n = 5$  in the fit). The caustic ring radius implied by the

image is 8.31 kpc, and its dimensions are  $p = 130$  pc and  $q = 200$  pc, in the directions parallel and perpendicular to the galactic plane respectively. It therefore predicts a rise which starts at 8.31 kpc and ends at 8.44 kpc, just where a rise is observed. Even if a rise were expected in the neighborhood, say randomly placed within a kpc of the triangular shape, the probability that its position agrees that closely with the position of the triangular shape is only of order  $10^{-3}$ .

In principle, the feature at  $(80^\circ, 0^\circ)$  should be matched by another in the opposite tangent direction to the nearby ring caustic, at approximately  $(-80^\circ, 0^\circ)$ . Although there is a plausible feature there, it is much less compelling than the one in the  $(+80^\circ, 0^\circ)$  direction. There are several reasons why it may not appear as strongly. One is that the  $(+80^\circ, 0^\circ)$  feature is in the middle of the Local spiral arm, whose stellar activity enhances the local gas emissivity, whereas the  $(-80^\circ, 0^\circ)$  feature is not so favorably located. Another is that the ring caustic in the  $(+80^\circ, 0^\circ)$  direction has unusually small dimensions. This may make it more visible by increasing its contrast with the background. In the  $(-80^\circ, 0^\circ)$  direction, the nearby ring caustic may have larger transverse dimensions.

Our proximity to a ring means that the associated flows, i.e. those flows in which the caustic occurs, contribute very importantly to the local dark matter density. Using the results of refs. <sup>9,12,14</sup>, and assuming axial symmetry of the caustic ring between us and the tangent point (approx. 1 kpc away from us), the densities and velocity vectors on Earth of the associated flows can be derived:

$$d^+ = 1.7 \cdot 10^{-24} \frac{\text{gr}}{\text{cm}^3}, \quad d^- = 1.5 \cdot 10^{-25} \frac{\text{gr}}{\text{cm}^3},$$

$$\vec{v}^\pm = (470 \hat{\phi} \pm 100 \hat{r}) \frac{\text{km}}{\text{s}}, \quad (6)$$

where  $\hat{r}$ ,  $\hat{\phi}$  and  $\hat{z}$  are the local unit vectors in galactocentric cylindrical coordinates.  $\hat{\phi}$  is in the direction of galactic rotation. The velocities are given in the (non-rotating) rest frame of the Galaxy. Because of an ambiguity, it is not presently possible to say whether  $d^\pm$  are the densities of the flows with velocity  $\vec{v}^\pm$  or  $\vec{v}^\mp$ .

Previous estimates of the local dark matter density, based on isothermal halo profiles, range from 5 to  $7.5 \cdot 10^{-25} \frac{\text{gr}}{\text{cm}^3}$ . The present analysis implies that a single flow ( $d^+$ ) has three times that much local density, i.e. that the total local density is four times higher than previously thought. The large size of  $d^+$  is due to our proximity to a cusp of the nearby caustic. Assuming axial symmetry, that cusp is only 55 pc away from us. The exact



size of  $d^+$  is sensitive to our distance to the cusp but, in any case,  $d^+$  is very large. If we are inside the tube of the fifth caustic, there are two additional flows on Earth, aside from those given in Eq. 6. A list of approximate local densities and velocity vectors for the  $n \neq 5$  flows can be found in ref. [21]. An updated list is in preparation.

The sharpness of the rises in the rotation curve and of the triangular feature in the IRAS map implies an upper limit on the velocity dispersion  $\delta v_{\text{DM}}$  of the infalling dark matter. Caustic ring singularities are spread over a distance of order  $\delta a \simeq \frac{R \delta v_{\text{DM}}}{v}$  where  $v$  is the velocity of the particles in the caustic,  $\delta v_{\text{DM}}$  is their velocity dispersion when they first fell in, and  $R$  is the turnaround radius then. The sharpness of the IRAS feature implies that its edges are spread over  $\delta a \lesssim 20$  pc. Assuming that the feature is due to the  $n = 5$  ring caustic,  $R \simeq 180$  kpc and  $v \simeq 480$  km/s. Therefore  $\delta v_{\text{DM}} \lesssim 53$  m/s.

The caustic ring model, and more specifically the prediction Eq. 6 of the locally dominant flow associated with the nearby ring, has important consequences for axion dark matter searches<sup>20</sup>, the annual modulation<sup>21,22,23</sup> and signal anisotropy<sup>25,24</sup> in WIMP searches, the search for  $\gamma$ -rays from dark matter annihilation<sup>26</sup>, and the search for gravitational lensing by dark matter caustics<sup>10,27</sup>. The model allows precise predictions to be made in each of these approaches to the dark matter problem.

### Acknowledgments

This work was supported in part by the US Department of Energy under grant No. DE-FG02-97ER41029.

### References

1. Axion reviews include: J.E. Kim, Phys. Rep. **150** (1987) 1; H.-Y. Cheng, Phys. Rep. **158** (1988) 1; R.D. Peccei, in 'CP Violation', ed. by C. Jarlskog, World Scientific Publ., 1989, pp 503-551; M.S. Turner, Phys. Rep. **197** (1990) 67; G.G. Raffelt, Phys. Rep. **198** (1990) 1.
2. P. Sikivie, Phys. Rev. Lett. **51** (1983) 1415 and Phys. Rev. **D32** (1985) 2988.
3. C. Hagmann et al., Phys. Rev. Lett. **80** (1998) 2043; S. Asztalos et al., Phys. Rev. **D64** (2001) 092003; S. Asztalos et al., Ap. J. **571** (2002) L27.
4. S. Matsuki and K. Yamamoto, Phys. Lett. **B263** (1991) 523; S. Matsuki, I. Ogawa, K. Yamamoto, Phys. Lett. **B336** (1994) 573; I. Ogawa, S. Matsuki and K. Yamamoto, Phys. Rev. **D53** (1996) R1740; K. Yamamoto et al., hep-ph/0101200.
5. K. Van Bibber, P. McIntyre, D. Morris and G. Raffelt, Phys. Rev. **D39** (1989) 2089.

6. Y. Inoue et al., Phys. Lett. **B536** (2002) 18.
7. K. Zioutas et al., NIM A425 (1999) 480.
8. P. Sikivie and J.R. Ipser, Phys. Lett. **B291** (1992) 288.
9. P. Sikivie, Phys. Lett. **B432** (1998) 139.
10. C. Hogan, astro-ph/9811290, to be published in Ap.J.
11. S. Tremaine, MNRAS **307** (1999) 877.
12. P. Sikivie, Phys. Rev. **D60** (1999) 063501.
13. J.A. Filmore and P. Goldreich, Ap.J. **281** (1984) 1; E. Bertschinger, Ap. J. Suppl. **58** (1985) 39.
14. P. Sikivie, I. Tkachev and Y. Wang, Phys. Rev. Lett. **75** (1995) 2911; Phys. Rev. **D56** (1997) 1863.
15. W. Kinney and P. Sikivie, Phys. Rev. **D61** (2000) 087305.
16. J. Binney and M. Merrifield, *Galactic Astronomy*, Princeton University Press, 1998, pp 550, 553.
17. D.P. Clemens, Ap.J. **295** (1985) 422.
18. D.B. Sanders et al., Ap.J.S. **60** (1986) 1; D.P. Clemens et al., Ap.J.S. **60** (1986) 297.
19. P. Sikivie, astro-ph/0109296.
20. C. Hagmann et al., Phys. Rev. Lett. **80** (1998) 2043; I. Ogawa, S. Matsuki and K. Yamamoto, Phys. Rev. **D53** (1996) 1740.
21. P. Sikivie, in the Proc. of the Second International Workshop on *The Identification of Dark Matter*, edited by N. Spooner and V. Kudryavtsev, World Scientific 1999, p. 68.
22. J. Vergados, Phys. Rev. **D63** (2001) 063511; A. Green, Phys. Rev. **D63** (2001) 103003; G. Gelmini and P. Gondolo, Phys. Rev. **D64** (2001) 023504.
23. P. Sikivie and S. Wick, Phys. Rev. **D66** (2002) 023504.
24. D. Stiff, L.M. Widrow and J. Frieman, Phys. Rev. **D64** (2001) 083516.
25. C. Copi, J. Heo and L. Krauss, Phys. Lett. **B461** (1999) 43.
26. L. Bergstrom, J. Edsjo and C. Gunnarsson, Phys. Rev. **D63** (2001) 083515; C. Hogan, astro-ph/0104106.
27. C. Charmousis, V. Onemli, Z. Qiu and P. Sikivie, in preparation.